Tanzania Journal of Engineering and Technology 2023, **42(2)**: 134-140
OPEN ACCESS articles distributed under Creative Commons Attribution Licence [CC BY-ND]
Websites: https://ajol.org/tjet; https://tjet.udsm.ac.tz

ISSN 1821-536X (**print**); ISSN 2619-8789 (**electronic**)
https://doi.org10.52339/tjet.v42i2.797

Regular Research Manuscript

Performance Evaluation of Full Array, Sub-Array and Overlapped-Sub-Array Hybrid BeamForming Architectures for Massive MIMO Systems

Godwin M. Gadiel

Department of Electronics and Telecommunication Engineering, College of Information and Communication Technologies, University of Dar es Salaam, P.O. Box 33335, Dar es Salaam, Tanzania

Corresponding author: gmruma@udsm.ac.tz; ORCID: https://orcid.org/0000-0003-0212-1466

ABSTRACT

The technological advancement in wireless communication, promises high data rate for end users. This has led to the possibility of smart cities, inter connected vehicles, and virtual reality applications. One of the recent technologies in wireless communication is massive MIMO where large number of antennas are deployed at the transmitter or receiver. This is possible due to the use of mmWave in wireless communication. With massive MIMO, beamforming technique can be employed in the communication system. Beamforming is the ability of communication system to direct power to the intended users and to cancel power at non-intended users and thus significantly improving communication system performance. Digital beamforming was initially used in MIMO systems. However, for massive MIMO systems it leads to high power consumption due to large number of dedicated radio frequency chain in each antenna. To address this challenge, hybrid beamforming techniques were introduced. There are three architectures for hybrid beamforming: Fully array architecture (FAA), overlapped sub-array architecture (OSA) and sub-array architecture (SAA). This paper has analysed three performance parameters of the mentioned hybrid beamforming architectures. The simulation results show that, FAA architecture has high performance in outage probability and spectral efficiency. However, its energy efficiency is lower compared to OSA and SAA. Specifically, SAA has the highest energy efficiency in comparison to FAA and OSA. It can also be observed that, with only 25% increased number of elements in OSA, the energy efficiency can be slightly lower compared to SAA, while achieving appreciable spectral efficiency performance with respect to FAA. Additionally, this work has derived an outage probability expression, which has not been covered in most of the studies. This study gives an insight of selecting the best architecture based on the performance requirement.

ARTICLE INFO

First submitted: Sept. 13, 2022

Revised: Dec. 20, 2022

Accepted: Apr. 19, 2023

Published: June, 2023

Keywords: *Massive MIMO, Hybrid beamforming, Energy efficiency, MU-MISO*

INTRODUCTION

Over several decades, wireless technology has advanced tremendously from first generation (1G) to recent development of fifth generation (5G) (Akpakwu et al.2017, Ayach et al., 2014). In the 5G, user can experience a data rate of more than 1 Gbps.

The ability of high data rate in 5G network, is enhanced by its physical layer, which embrace massive MIMO and beamforming. Beamforming is the ability of directing power to the intended user, by taking advantage of massive antenna elements at the transmitter (Ayach et al. 2012). In the beginning, beamforming was realized by a digital processor and multiple radio frequency (RF) chains which were connected to each antenna (Mendez-Rial et al. 2016). This set up was known as digital beamforming. However, in massive MIMO, this set up is almost impossible, because, RF chains are power hungry devices and in massive MIMO the number of antennas is large.

In order to overcome this drawback, researchers proposed a hybrid beamforming architecture, where an analogue beamforming architecture was combined with digital beamforming architecture. Hybrid beamforming architecture (HBA) takes advantage of high data rate provided by digital beamforming and low power consumption provided by analogue beamforming architecture. In the hybrid beamforming architecture, there are three most commonly used architectures. These are: Fully array architecture (FAA) in which all RF chain is connected to all antennas via phase shifters. Overlapped subarray architecture (OSA) in which an RF chain is connected to a set of antennas, whereby some sets of antennas are connected to more than one RF chain. Lastly, subarray architecture (SAA) where each RF chain is connected to a strict sub set of antenna (Abbaspour-tamijani et al. 2003, Mendez-Rial et al. 2016).

Many researchers, have discussed these architectures, showing its performance characteristics in different environment. In (Ahmed et al. 2018), it was realized that FAA can approach an optimal performance in terms of spectral efficiency. Even though the spectral efficiency performance of OSA presented in (Song et al. 2017) is lower than FAA, it has advantages of power consumption due to fewer number of phase shifters compared to FAA. SAA has low spectral performance, but it has the least power consumption, as the number of phase shifters is reduced to N_t.

Beside the performance comparison architectural differences mentioned earlier, there is no work to the best of authors knowledge, that analyzed the performance of the three architectures under the same environment (Wan et al. 2021). This work, intend to analyse the spectral efficiency, energy efficiency and outage probability for the three architectures. This work uses the beamforming technique used in (Liang et al. 2014) to analyze the performance of the three architecture in multi-user multiple input single output (MU-MISO) system. The main contribution of this work, is the single analysis that give a trade-offs between the three architectures in terms of spectral efficiency, energy efficiency and outage probability.

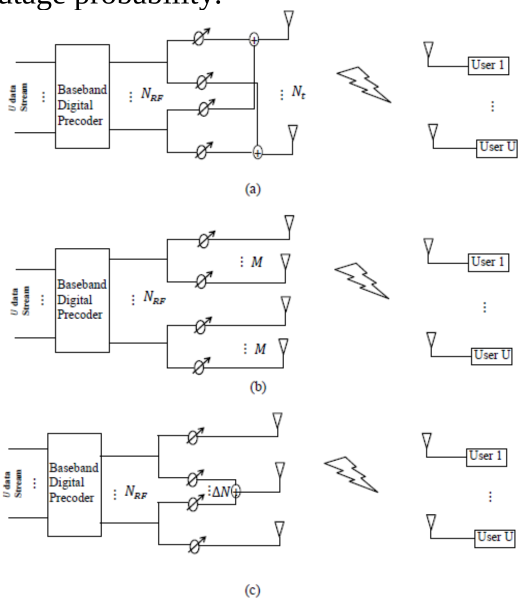

Figure 1: Hybrid beamforming architectures (a) Fully array architecture, (b) Sub array architecture, and (c) Overlapped sub-array architecture.

METHODS AND MATERIALS

This work used mathematical methods and simulation to analyse the performance of three hybrid beamforming architectures. This section, presents the system model and outage probability analysis. The details of each is presented in the next subsections.

System model

In this work, a MU-MISO system is considered, where a base station (BS) with N_t antennas and N_{RF} chain is transmitting data to K multiple users each with single antenna. In the downlink transmission, K symbols sent to each user, the corresponding symbol is multiplied by a digital precoder f_{BB}^{k}, then converted to RF domain by RF chains before being precoded by RF precoder F_{RF} of dimension $N_t \times N_{RF}$. The received signal at user k can be written as Equation (1) which is

$$y_k = h_k^H F_{RF} f_{BB}^k s_k + n_k \tag{1}$$

where h_k^H denotes the channel between the BS and $k-th$ user, s_k is the symbol for the $k-th$ user such that $s_k s_k^* = 1$ and n_k is the noise for user k that is independent and identically distributed (i.i.d), which follows the complex Gaussian distribution $\mathcal{CN}(0,\sigma^2)$.

The RF precoder structure for FAA, SAA and OSA are as defined in Equations (2), (3) and (4) respectively (Wong et al. 2021, Zhao et al. 2021, Busari et al. 2019).

$$F_{RF}^{FA} = \begin{bmatrix} f_{(1,1)}^{FA} & \cdots & f_{1,K}^{FA} \\ \cdot & \cdot & \cdot \\ \cdot & \cdot & \cdot \\ \cdot & \cdot & \cdot \\ f_{(N_t,1)}^{FA} & \cdots & f_{(N_t,K)}^{FA} \end{bmatrix} \tag{2}$$

$$F_{RF}^{SA} = \begin{bmatrix} f_1^{SA} & 0 & 0 & 0 \\ 0 & f_2^{SA} & 0 & 0 \\ 0 & 0 & \ddots & 0 \\ 0 & 0 & 0 & f_K^{SA} \end{bmatrix} \tag{3}$$

where f_k^{SA} is the $M \times 1$ weighting vector for the k th subarray and $M = {N_t}/{K}$,

$$F_{RF}^{OS} = \begin{bmatrix} f_1^{OS}(1) & 0 & & 0 \\ \vdots & f_2^{OS}(1) & & 0 \\ f_1^{OS}(N) & \vdots & \ddots & 0 \\ 0 & f_2^{OS}(N) & & f_K^{OS}(1) \\ 0 & 0 & & \vdots \\ 0 & 0 & & f_K^{OS}(N) \end{bmatrix} \tag{4}$$

where N is the number of phase shifters connected to a subarray. The inter-subarray distance is defined as ΔN, with respect to the number of antennas, which is the number of overllaped elements between adjacent RF chains. This parameter range from $\Delta N = 0$, where OSA becomes FAA and $\Delta N = M$, where OSA becomes SA. The element of RF precoder is as defined in (Liang et al. 2014)), and it is given by $f_{(i,k)}^{FA} = \frac{1}{\sqrt{N_t}} e^{-j\theta_{(i,k)}}$, $f_{(i,k)}^{SA} = \frac{1}{\sqrt{M}} e^{-j\theta_{(i,k)}}$ and $f_{(i,k)}^{OS} = \frac{1}{\sqrt{N}} e^{-j\theta_{(i,k)}}$, for FA, SA, OS architectures. Where, $\theta_{(i,k)} = \angle[H]_{(i,k)}$ for phase shifter with infinite resolution.

Outage probability analysis

In this section, a statistical analysis of the SINR formulated in the previous section is done. Specifically, the outage probability analysis of the uth MS based on transmitt beamforming from the three architectures is performed. Based on analysis of (Liang et al. 2014), the main diagonal elements following the central limit theorem and zero forcing is used in digital precoding is given by Equation (5).

$$h_k^H f_k \sim \mathcal{N}\left(\frac{\sqrt{\pi N_t}}{2}, 1 - \frac{\pi}{4}\right) \tag{5}$$

For the case of off-diagonal elements, with similar assumption that zero force is used in digital precoding, i.e $j \neq k$ we have Equation (6).

$$h_k^H f_j \sim \mathcal{CN}(0,1) \tag{6}$$

From the results in equatin (5) and (6), the SINR is upper bounded by the Equation (7).

$$SINR \cong \frac{P}{\sigma^2} \left|h_k^H f_k\right|^2 \tag{7}$$

By defining the random variable $X_u = |h_k^H f_k|^2$, then (6) can be written as Equation (8).

$$SINR \cong \frac{P}{\sigma^2} X_u \tag{8}$$

From the exressin in, and the assumption h element defined earlier, the outage probability of the uth mobile station is given by Equation (9) (Tse and Viswanath 2012).

$$P_{out}^{u}(R) = 1 - \exp(\frac{-(2^R - 1)}{PX_u}\sigma^2) \quad (9)$$

Since X_u follows the distribution of the main diagonal element (Feng et al. 2016), therefore, considering it mean power, the outage probability can be re-defined to the following expression (Equation (10)).

$$P_{out}^{u}(R) = 1 - \exp(\frac{-(2^R - 1)}{P\pi N_t}4\sigma^2) \quad (10)$$

RESULTS AND DISCUSSION

In this section, system sum rate, energy efficiency and outage probability are numerically analized for the three architectures. The simulation considers an environment where the channel coefficiency between the base station and uth user is characterized by the geometric Saleh-Valenzuela channel model (Nguyen and Lee 2019, Huang et al. 2020). This model is commonly used in massive MIMO communication systems. In this case, the channel vector between the base station and uth user is given by Equation (11).

$$h_u = \sqrt{\frac{N_t}{L_u}}\sum_{l=1}^{L_u}\alpha_{u,l}a_{BS}(\emptyset_{u,l}) \quad (11)$$

The L_u is the number of effective channel paths corresponding to limited number of scatters between the BS and the uth MS, $\alpha_{u,l}$ is the channel gain which is assumed to be i.i.d Gaussian random variable with zero mean and unit variance, and $\emptyset_{u,l} \in [0,2\pi]$ is the azimuth angle of departure (AoD) of the lth path. Whereas, a_{BS} represents the normalized transmit array respense vector at the BS that depends on the structure of the antenna array. Particularly, this work has considered a uniform linear array (ULA) where the array response vector is given by Equation (12).

$$a(\emptyset) = \frac{1}{\sqrt{N_t}}\left[\begin{matrix}1, e^{j\frac{2\pi}{\lambda}dsin(\emptyset)}, \dots \\ , e^{j(N_t-1)\frac{2\pi}{\lambda}dsin(\emptyset)}\end{matrix}\right]^T \quad (12)$$

where λ denotes the wavelength of the signal and $d = \lambda/_2$ is the antenna spacing in the antenna array(Ayach et al. 2014). In this work, the signal to noise ratio (SNR) is defined as the ratio of the common average SNR received at each antenna with noise variance normalized to unity.

Figure 2 presents the outage probability versus the achievable rate. When the number of bits increases per channel use, the outage probability increases.

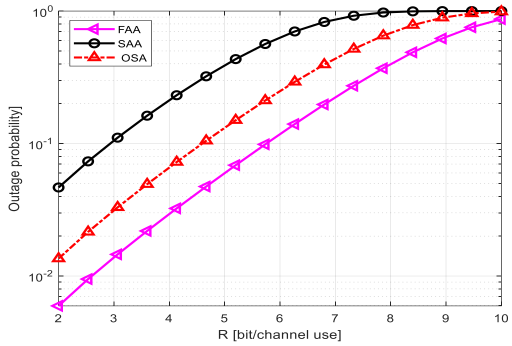

Figure 2: Outage probability versus number of bits per channel (SNR = 10 dB).

The FAA has the lowest outage probability throughout the performance range, followed by OSA, and SAA has the lowest performance. Specifically, when the number of bits per channel use is 6, the FAA achieves an outage probability of 0.1, while that of OSA achieves an outage probability of 0.21, and SAA achieves an outage probability of 0.7.

Figure 3 shows the outage probability versus signal to noise ratio, when the bits per channel use is 8. FAA has the lowest outage probability throughout the entire SNR range, followed by OSA, and finally SAA. It is observed that, by increasing the number of overlapping antenna elements to 12, from the original SAA, the OSA has managed to improve the outage probability significantly. In Figure 4, a comparison between different architectures and their achievable system sum rate is presented. The FAA achieves the performance near the digital beamforming architecture, which provide the optimal precoding. OSA has a performance higher than SAA by increasing 12 elements in the overlapped subarray.

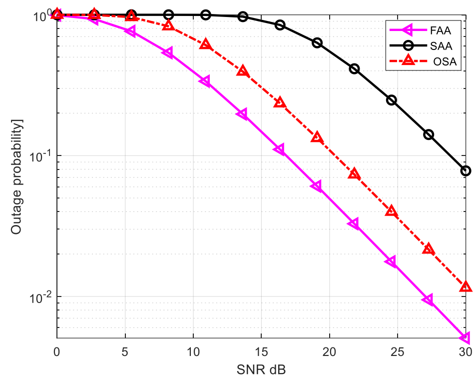

Figure 3: Outage probability versus SNR (R = 8 bits/channel use, U = 16).

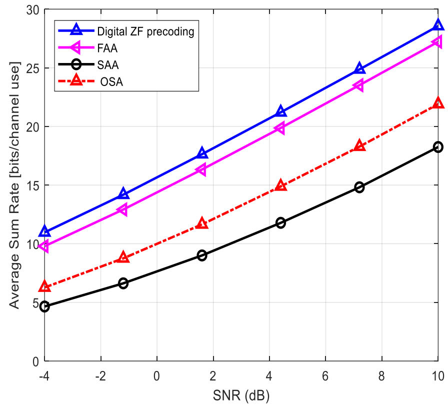

Figure 4: System sum rate versus SNR (Nt = 64 and U = 4).

The performance can be further improved if additional elements are utilized. Figure 5 plots the spectral efficiency versus the number of users, which is equivalent to number of RF chains in this simulation results. The results show that, FAA has high performance in comparison with OSA and SAA. It is also observed that, OSA has improved the spectral efficiency in comparison to SAA.

In Figure 6, the simulation results of the three architectures are presented, where the achieved spectral efficiency is observed as the number of antennas increases. In this simulation, it was assumed the number of users are 4, which is equal to the number of RF chains. It is observed that, the FAA has high performance in comparison to OSA and SAA. For the case of OSA, the number of phase shifters was kept to only 25% higher than that of SAA. The results show that, slightly increase of phase shifter can significantly improve the spectral efficiency. Lastly, the paper analyse the energy efficiency of the three architectures in the simulation results presented in Figure 7. It is observed that, as the number of antennae increases, the energy efficiency decreases for both architectures.

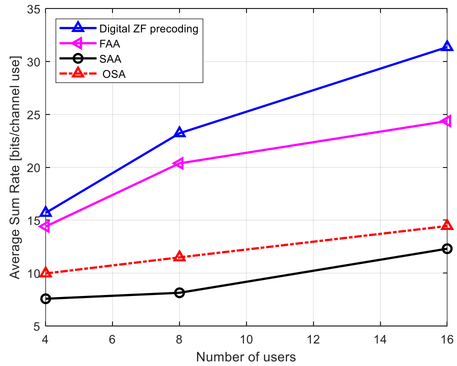

Figure 5: System sum rate versus number of users (SNR = 0 dB).

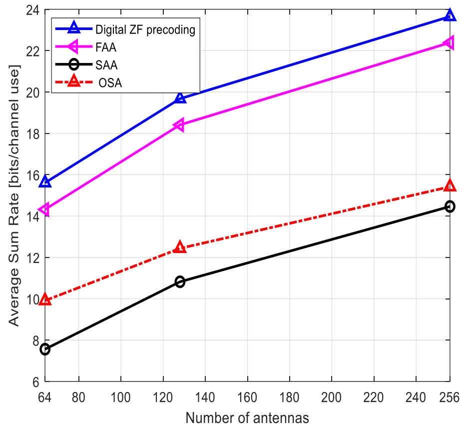

Figure 6: System sum rate versus number of antennas (SNR = 0 dB).

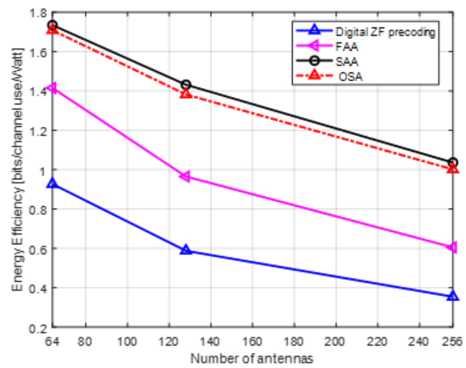

Figure 7: Energy Efficiency vers number of antennas (SNR = 0 dB).

This is due to the fact that, as the number of antenna increases, the number of phase shifters also increases. Additionally, the results show that, SAA has the highest energy efficiency compared to OSA and FAA. It is noted that, the energy efficiency of OSA is slightly lower compared to SAA. With this observation, OSA can be a potential candidate where spectral efficiency and energy efficiency are of concern.

CONCLUSION AND RECOMMENDATIONS

Hybrid beamforming is an enabling technology in massive MIMO systems, which enhance data rates in wireless communication. This paper has analysed the performance of the three hybrid beamforming architectures: fully array architecture, overlapped sub-array architecture, and sub-array architecture. The simulation result show that, the FAA has the highest performance in outage probability and spectral efficiency. SAA has high performance in energy efficiency, however, it performs poorly in both spectral efficiency and outage probability. Furthermore, it has been demonstrated that OSA has intermediate performance between the two. With these results, it is possible to select between the three architectures based on performance requirements. This work will be expanded in the future to include derived architectures such as un-equal subarray architecture and dynamic un-equal subarray architecture. Additionally, a point-to-point scenario will also be considered, and the bit error rate performance parameter will be analyzed in a point-to-multi-point scenario.

REFERENCES

Abbaspour-tamijani, Abbas, and Kamal Sarabandi. 2003. “An Affordable Millimiterwave Beam-Steerable Antenna Using Interleaved Planar Subarrays.” *IEEE Transactions on Antennas and Propagation*, 51(9): 2193-2202, https://doi.org/10.1109/TAP.2003.816331

Ahmed, Irfan, Hedi Khammari, Adnan Shahid, Ahmed Musa, Kwang Soon Kim, Eli De Poorter, and Ingrid Moerman. 2018. “A Survey on Hybrid Beamforming Techniques in 5G: Architecture and System Model Perspectives.” *IEEE Communications Surveys and Tutorials*, 20 (4): 1–40. https://doi.org/10.1109/COMST.2018.2843719.

Akpakwu, Godfrey Anuga, Bruno J Silva, Gerhard P Hancke, and Adnan M Abu-Mahfouz. n.d. “A Survey on 5G Networks for the Internet of Things: Communication Technologies and Challenges.” *IEEE Access* 6: 3619–47. https://doi.org/10.1109/ACCESS.2017.2779844.

Ayach, Omar El, Robert W Heath, Shadi Abu-Surra, Sridhar Rajagopal, and Zhouyue Pi. 2012. “Low Complexity Precoding for Large Millimeter Wave MIMO Systems.” *IEEE Int. Conf. Commun.*, 3724–29. https://doi.org/10.1109/ICC.2012.6363634.

Ayach, Omar El, Sridhar Rajagopal, Shadi Abu-Surra, Zhouyue Pi, and Robert W. Heath. 2014. “Spatially Sparse Precoding in Millimeter Wave MIMO Systems.” *IEEE Transactions on Wireless Communications* 13 (3): 1499–1513. https://doi.org/10.1109/TWC.2014.011714.130846.

Busari, Sherif Adeshina, Kazi Mohammed Saidul Huq, Shahid Mumtaz, Jonathan Rodriguez, Yi Fang, Douglas C. Sicker, Saba Al-Rubaye, and Antonios Tsourdos. 2019. “Generalized Hybrid Beamforming for Vehicular Connectivity Using THz Massive MIMO.” *IEEE Transactions on Vehicular Technology* 68 (9): 8372–83. https://doi.org/10.1109/TVT.2019.2921563.

Feng, Chi, Yindi Jing, and Shi Jin. 2016. “Interference and Outage Probability Analysis for Massive MIMO Downlink with MF Precoding.” *IEEE Signal Process. Lett.* 23 (3): 366–70.

https://doi.org/10.1109/LSP.2015.2511630.

Huang, Shaocheng, Yu Ye, and Ming Xiao. 2020. "Hybrid Beamforming for Millimeter Wave Multi-User MIMO Systems Using Learning Machine." *IEEE Wireless Communications Letters* 9 (11): 1914–18. https://doi.org/10.1109/LWC.2020.3007990.

Liang, Le, Wei Xu, and Xiaodai Dong. n.d. "Low-Complexity Hybrid Precoding in Massive Multiuser MIMO Systems." *IEEE Wirel. Commun. Lett.* 3 (6): 653–56. https://doi.org/10.1109/LWC.2014.2363831.

Mendez-Rial, Roi, Cristian Rusu, Nuria Gonzalez-Prelcic, Ahmed Alkhateeb, and Robert W. Heath. 2016. "Hybrid MIMO Architectures for Millimeter Wave Communications: Phase Shifters or Switches?" *IEEE Access* 4: 247–67. https://doi.org/10.1109/ACCESS.2015.2514261.

Nguyen, Nhan Thanh, and Kyungchun Lee. 2019. "Unequally Sub-Connected Architecture for Hybrid Beamforming in Massive MIMO Systems," 1–11. http://arxiv.org/abs/1908.10056.

Song, Nuan, Tao Yang, and Huan Sun. 2017. "Overlapped Subarray Based Hybrid Beamforming for Millimeter Wave Multiuser Massive MIMO." *IEEE Signal Processing Letters* 24 (5): 550–54. https://doi.org/10.1109/LSP.2017.2681689.

Tse, David, and Pramod Viswanath. 2012. "Capacity of Wireless Channels." *Fundamentals of Wireless Communication*, 166–227. https://doi.org/10.1017/cbo9780511807213.006.

Wan, Shaojun, Hongbin Zhu, Kai Kang, and Hua Qian. 2021. "On the Performance of Fully-Connected and Sub-Connected Hybrid Beamforming System." *IEEE Transactions on Vehicular Technology* 70 (10): 11078–82. https://doi.org/10.1109/TVT.2021.3109300.

Wong, Sin Sheng, Chieh Fang Teng, and An Yeu Wu. 2021. "Two-Step Codebook-Assisted Alternating Minimization (CA-AltMin) for Low-Complexity Hybrid Beamforming Design." *IEEE Communications Letters* 25 (6): 1989–93. https://doi.org/10.1109/LCOMM.2021.3061884.

Zhao, Xingyu, Tian Lin, Yu Zhu, and Jun Zhang. 2021. "Partially-Connected Hybrid Beamforming for Spectral Efficiency Maximization via a Weighted MMSE Equivalence." *IEEE Transactions on Wireless Communications* 1276 (c): 1–15. https://doi.org/10.1109/TWC.2021.3091524